

Prediction of Solidification Behavior of Al Alloy in a Cube Mold Cavity

N. P. Yadav, Deepti Verma

Abstract---This paper focuses on the mathematical modeling for solidification of Al alloy in a cube mold cavity to study the solidification behavior of casting process. The parametric investigation of solidification process inside the cavity was performed by using computational solidification/melting model coupled with Volume of fluid (VOF) model. The implicit filling algorithm is used in this study to understand the overall process from the filling stage to solidification in a model metal casting process. The model is validated with past studied at same conditions. The solidification process is analyzed by including the effect of pouring velocity as well as natural convection from the wall and geometry of the cavity. These studies show the possibility of various defects during solidification process.

Keywords---Buoyancy driven flow, natural convection driven flow, residual flow, secondary flow, volume of fluid.

I. INTRODUCTION

THE casting process is one of the important manufacturing processes. This process is widely used to produce metal components. Therefore, various researchers are devoted toward process development for the production of high quality casting goods at low costs. The macroscopic point of view, casting processes involve the coupling of solidification heat transfer and fluid flow. Therefore, the solidification and heat transfer as well as fluid flow phenomenon have key role in casting of material because the material structure as well as mechanical properties of the material is affected by them.

The casting process is required to pour the material in the mold. The different flow mechanisms are involved during these processes. Im et al. [1] have discussed the simultaneous filling and solidification in two-dimensional square cavity. The different mechanisms involved during the process are as follows: (i) mold filling through the gating system (ii) residual flow due to the incoming momentum and (iii) natural-convection-driven flow in the mold can be considered during the casting process. The most common defect in aluminum permanent mould casting is porosity. Swaminathan and Voller [2] have studied a general implicit source based enthalpy method to deal with the problem that has metallurgical solidification. This method can use for wide range of enthalpy temperature relationship. Chen et al. [3] have studied the solidification behavior of pure aluminum in a square enclosure in both, with and without the inclusion of natural convection effects in the liquid zone. The convection has a significant

effect on the formation of the solid/liquid interface. Swaminathan and Voller [4] have studied the volume of fluid (VOF) method to track the liquid /air interface during the filling. The previous VOF method is explicit in nature and has time step restriction. Pathak et al. [5] have discussed the couple effect generated by the filling process in buoyancy-driven flow and the residual flow. The solidification behavior was studied by carrying out a numerical study for simultaneous mold filling and solidification of a pure metal.

Jadayil [6] has studied the effect of pouring rate on Aluminum cast. As the pouring rate of the molten material increased the more surface defects in the casting is observed while less internal (subsurface) defects are found in the casting for the same. Vander [7] has studied the effects of solidification rate on the microstructure of the cast aluminum alloy A356. As the solidification rate increases the number of pores increased and decreased the size of pore and the volume fraction of porosity. Kakas et al. [8] have studied the porosity defect in aluminum casting. It is concluded that the numerical simulation detected the areas in which porosity defect occurs. These defects get eliminated by changing the gate dimension.

Gopinath and Balanarasimman [9] have studied the casting process to cast a plate with the combination of different riser dimensions. The simulation of solidification process was made with ANSYS software. The solidification time and optimal riser diameters are validated with experimental results. Kim and Kaviany [10] have discussed a fully implicit method for diffusion controlled solidification problem. Rady and Mohanty [11] have applied an enthalpy porosity technique to solve the solidification and melting problem in a rectangular technique. Kuo et al. [12] have discussed one-dimensional heat transfer system for the casting to the mold. They observe it for fully molten metal and semi-solid metal. Akihiko and Yasunori [13] have discussed the effect of backpressure on mold filling behavior. The simulation code was generated to consider the backpressure by direct difference method. Nguyen and Huang [14] have studied the effect of inlet velocity on cooling wall inlet velocity is low. The increase in the cooling wall temperature and inlet velocity is the best way to decrease the turbulence phenomenon in casting process. The thermal arrest time take longer time due to strong turbulence flow. The optimum cooling wall temperature and inlet velocity are importance parameters to reduce the time of thermal arrest and turbulence flow in casting process. Crowley and Ockedon [15] have done numerical solution to solve the solidification problem in casting process. In this method, the equation of heat and mass transfer are combined at moving phase boundary. Mbaye and Bilgen [16] have used a finite difference

N. P. Yadav, Deepti Verma are with the Bundelkhand Institute of Engineering. &Technology, Jhansi, Uttar Pradesh, 284128, India (phone: 9415684455; e-mail: npy_biet@rediffmail.com, vermadeepti27@gmail.com).

control volume method to study the melting of a pure metal in a rectangular cavity by natural convection method.

This paper focuses the mathematical modeling for solidification of liquid material in a mould cavity to understand the solidification behavior in the casting process. The pouring velocity as well as natural convection from the wall of the cavity is considered to investigation of solidification process inside the cavity. The numerical simulation of solidification process inside the cavity is performed by using computational solidification/melting model package ANSYS FLUENT coupled with VOF model. The effects of different parameters on solidification process are carried out by the behavior of temperature, velocity and liquid fraction profiles during solidification with time.

II. MATHEMATICAL MODELING

A. Solidification Model

This model can be used to solve fluid flow problems involving solidification and/or melting taking place at one temperature (e.g., in pure metals) or over a range of temperatures (e.g., in binary alloys). This model uses an enthalpy-porosity formulation.

1. Energy Equation

The enthalpy (H) of the material is computed as the sum of the sensible enthalpy, h, and the latent heat, ΔH:

$$H = h + \Delta H \quad (1)$$

$$h(\text{Sensible Enthalpy}) = h_{ref} + \int_{T_{ref}}^T C_p dT \quad (2)$$

where; h_{ref} = reference enthalpy, T_{ref} = reference temperature, C_p = specific heat at constant pressure.

The energy equation in solidification/melting problems is written as:

$$\frac{\partial(\rho H)}{\partial t} + \nabla \cdot (\rho v H) = \nabla \cdot (k \nabla T) + S \quad (3)$$

where; H = enthalpy, ρ = density, v = fluid velocity, S = source term, k = thermal conductivity.

2. Momentum Equation

The momentum sink due to the reduced porosity in the mushy zone takes the following form:

$$s = \frac{(1-\beta)^2}{(\beta^3 - \epsilon)} A_{mush} (v - v_p) \quad (4)$$

where; β = liquid volume fraction, ϵ = small number (0.001) to prevent division by zero A_{mush} = mushy zone constant, v_p = solid velocity due to the pulling of solidified material out of the domain.

3. Model of Liquid Fraction

The liquid fraction (β) can be calculated as in (5) suggested by [17]:

$$\beta = \frac{T - T_{solidus}}{T_{liquidus} - T_{solidus}} \quad (5)$$

$$\beta = 0 \quad \text{if } T < T_{solidus}$$

$$\beta = 1 \quad \text{if } T > T_{liquidus}$$

The latent heat content (ΔH) can now be written in terms of the latent heat of the material L as:

$$\Delta H = \beta L \quad (6)$$

where; L is latent heat of the material.

4. Turbulence Model

The sinks are added to all of the turbulence equations in the mushy and solidified zones to account for the presence of solid matter [17].

$$s = \frac{(1-\beta)^2}{(\beta^3 + \epsilon)} A_{mush} \varphi \quad (7)$$

where; φ represents the turbulence quantity being solved (k, ϵ , ω , etc.), and the mushy zone constant, A_{mush} is the same as the one used in momentum equation.

5. Modeling of Contact Resistance at Wall

The wall heat flux (q) can be calculated as given in [17]:

$$q = \frac{T - T_w}{\left(\frac{l}{k} + R_c(1-\beta)\right)} \quad (8)$$

where T = temperature at any point within the cell, T_w = wall temperature, l = distance between the wall and the point and R_c = the contact resistance, which has the same units as the inverse of the heat transfer coefficient.

B. Modeling of Volume of Fluid (VOF)

The VOF model can model two or more immiscible fluids by solving a single set of momentum equations and tracking the volume fraction of each of the fluids throughout the domain. The q_{th} fluid's volume fraction in the cell is denoted as a_q , then the following three conditions are possible[1]:

- $a_q = 0$: The cell is empty (of the q_{th} fluid)
- $a_q = 1$: The cell is full (of the q_{th} fluid)
- $0 < a_q < 1$: The cell contains the interface between the q_{th} fluid and one or more other fluids.

1. Modeling of Volume Fraction

The tracking of the interface(s) between the phases is accomplished by the solution of a continuity equation for the volume fraction of one (or more) of the phases. For the q_{th} phase, this equation has the following form:

$$\frac{1}{\rho_q} \left[\frac{\partial}{\partial t} (a_q \rho_q) + \nabla \cdot (a_q \rho_q v_q) \right] = s_{a_q} + \sum_{p=1}^n (m_{pq} - m_{qp}) \quad (9)$$

where; m_{qp} = mass transfer from phase q to phase p and m_{pq} = mass transfer from phase p to phase q

The time discretization was done on the implicit scheme based, the standard finite-difference interpolation schemes,

QUICK, Second Order Upwind and First Order Upwind, and the Modified HRIC schemes, are used to obtain the face fluxes for all cells, including those near the interface.

2. Momentum Equation

A single momentum equation is solved throughout the domain, and the resulting velocity field is shared among the phases. The momentum equation, shown in equation (10), is dependent on the volume fractions of all phases through the properties density (ρ) and viscosity (μ).

$$\frac{\partial}{\partial t}(\rho v) + \nabla \cdot (\rho v v) = -\nabla P + \nabla \cdot [\mu(\nabla v + \nabla v^T)] + \rho g + F \quad (10)$$

where; F is external body force.

3. Energy Equation

The energy equation, also shared among the phases, is shown as:

$$\frac{\partial}{\partial t}(\rho E) + \nabla \cdot (v(\rho E + P)) = \nabla \cdot (k_{\text{eff}} \nabla T) + S_h \quad (11)$$

where; P is the static pressure, S_h is heat source and k_{eff} is effective thermal conductivity. The VOF model treats energy, E, and temperature, T, as mass-averaged variables:

$$E = \frac{\sum_{q=1}^n a_q \rho_q E_q}{\sum_{q=1}^n a_q \rho_q} \quad (12)$$

where; E_q for each phase is based on the specific heat of that phase and the shared temperature.

III. NUMERICAL SIMULATION

The governing equations along with the other modeling equations have been solved using a computational solidification/melting model package called ANSYS FLUENT (Version 14.0). The numerical solution of governing equations includes three steps: (a) A grid arrangement to divide the domain of interest into discrete elements, (b) Discretization and derivation of the algebraic analogues of the equations by a numerical scheme and (c) Solution of the resulting algebraic equations by a matrix solver. The method of nodal point integration (NPI) is employed for the integration of the governing differential equations over each control volume (element) of the physical domain. The resulting matrix of algebraic equations is solved by using the implicit method. For all variables of mass, velocity components and turbulence quantities the convergence criteria are set as the normalized total overall residue value which is equal to 10^{-3} . The complete domain is discretized into a structured grid as shown in Fig. 1. A finer grid size has been selected in region, for obtaining good accuracy in the predicted solution.

The unified algorithm for simultaneous filling and solidification is applied to the mold shown in Fig. 2 as discussed by [1] is used for grid independence test. The liquid metal enters through the gate at the right-hand corner of the top wall, and the other walls are insulated except the left wall (to initiate the solidification). The left wall temperature is

maintained at 773 K throughout the process and the gate velocity is 0.1 m/s. The material used for solidification is AL alloy and its thermophysical properties and operating condition are shown in Tables I and II, respectively.

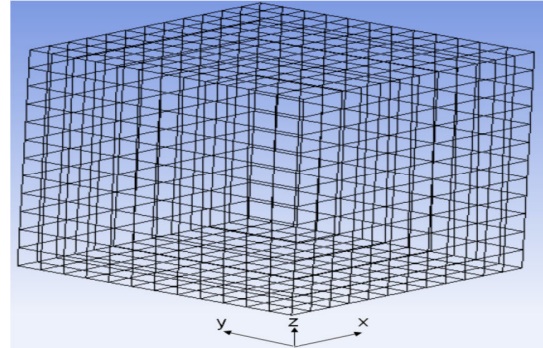


Fig. 1 Grid pattern for the geometry considered in the present study

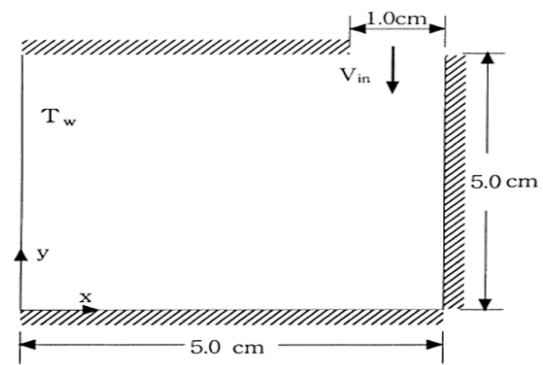


Fig. 2 Cube mold cavity [1]

TABLE I
 THERMOPHYSICAL PROPERTIES OF ALUMINUM ALLOY [1]

Conductivity, k	100.0 W/mK
Specific heat, c	1000.0 J/kgK
Density, ρ	2500.0 kg/m ³
Liquidus temperature, T_l	650.0°C
Solidus temperature, T_s	550.0°C
Latent heat, h	400.0 kJ/kg
Viscosity, μ	0.0025 kg/m/s

TABLE II
 OPERATING CONDITION

Pouring velocity, v_i	0.1 m/s
Pouring temperature, T_i	973 K
Left wall temperature, T_{wl}	773 K

Fig. 3 shows the temperature contour for different nodes 2197, 14400 and 68921 related to the same geometry of the mold as in Fig. 2. As it can be seen that the results for 2197 grid size is similar to the one for 14400. Therefore the grid convergence has been achieved for this geometry. Hence, the use of 2197 and 14400 node value is more accurate than the 68921 node. Based on the grid independence criterion the grid of 14400 sizes is chosen for further analysis.

IV. BOUNDARY CONDITION

The geometry used in this study is shown in Fig. 1. A detailed description of the boundary conditions applied is given below: (a) At the inlet: $u = U_0$ and $v = 0$, (b) On the wall, the no-slip condition ($u=v=0$) is specified on velocity along with $\frac{\partial p}{\partial n} = 0$ and (c) At Bottom wall: heat flux=0 and temperature=300 K, free convection. At the inlet, turbulence

level is specified in terms of percentage turbulence intensity. The relationship between the turbulent kinetic energy (k) and turbulence intensity (I) is given by (13).

$$k = \frac{3}{2} (u_{avg} I)^2 \quad \text{where} \quad I = \frac{\sqrt{\frac{1}{2} (u'^2 + v'^2)}}{u_{avg}} \quad (13)$$

where u_{avg} is the mean flow velocity.

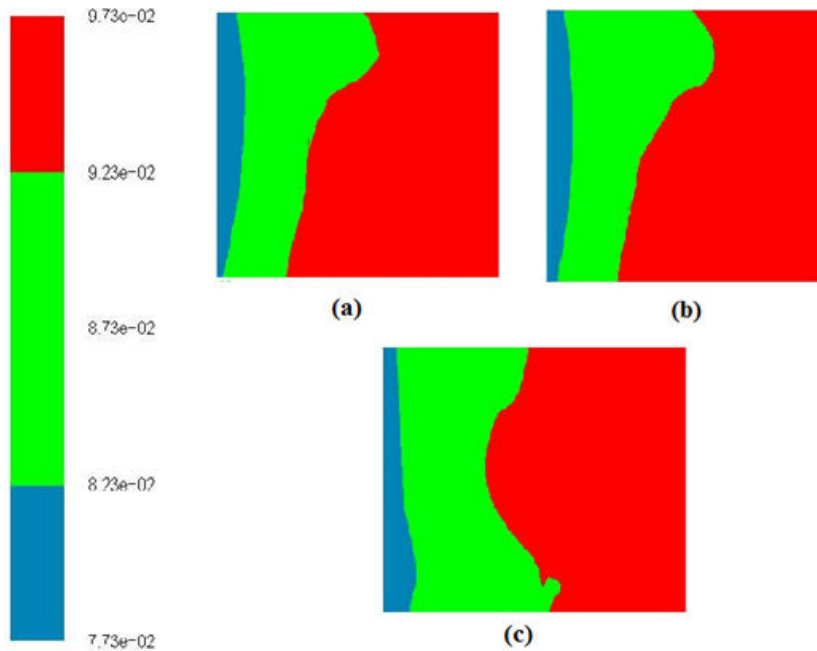


Fig. 3 Temperature contour for different node (a) 2197 (b) 14400 and (c) 68921

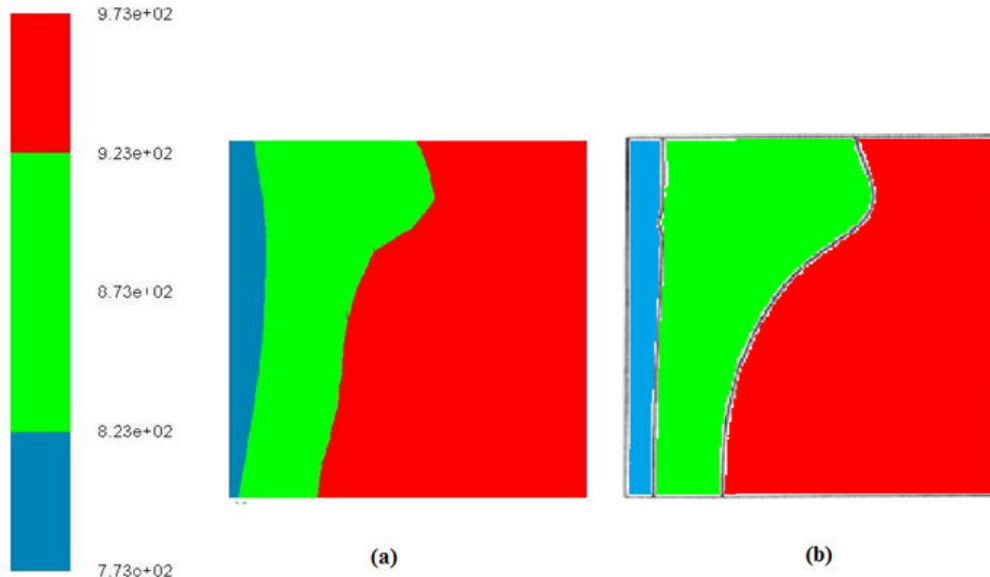


Fig. 4 Temperature contour for (a) present study and (b) Im et al. [1] study

V. VALIDATION OF THE CODE

The model was benchmarked by simulating the flow conditions described and compare the temperature contour

obtained by [1] with the present study. The complete solidification domain is discretized into a structured grid as shown in Fig. 1. A grid independence test has been performed at thermo-physical properties of metal as in Table I. The

variation of temperature study for solidification for present study and [1] was done at same conditions and the results are shown in Fig. 4. Although not much variation was noticed for

14400 nodes, the grid is chosen for further simulations in order to resolve steep gradients for obtaining good accuracy in the predicted solution.

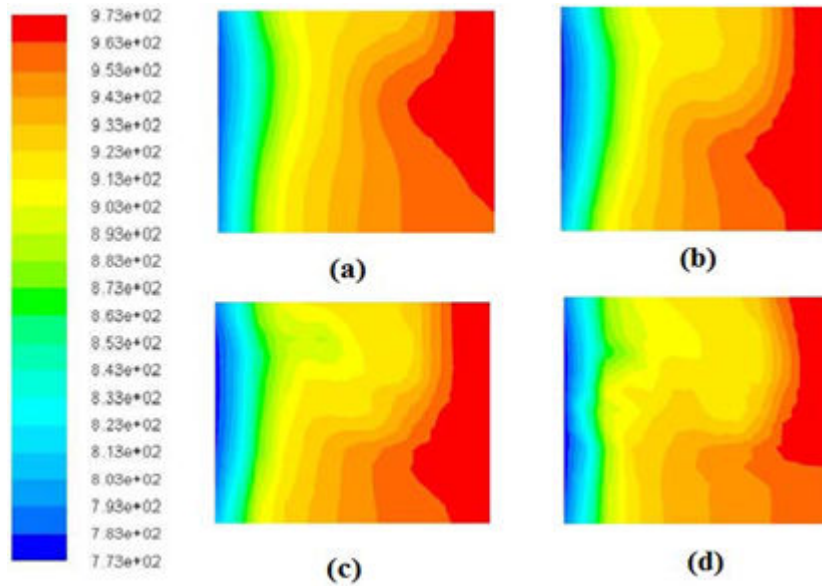


Fig. 5 Temperature contour at different inlet velocity for $t = 10$ sec, $T_i = 973$ K, $T_{wl} = 773$ K, $h_g = 5$ cm and filling at the right side of the top plane: (a) 0.05 m/s, (b) 0.1 m/s, (c) 0.15 m/s and (d) 0.2 m/s

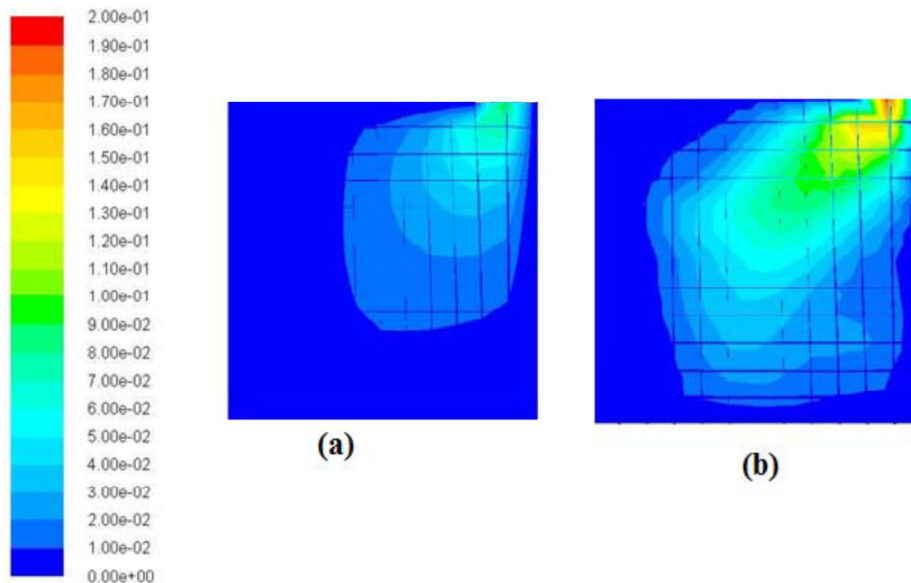


Fig. 6 Velocity contour at different inlet velocity for $t = 10$ sec, $T_i = 973$ K, $T_{wl} = 773$ K, $h_g = 5$ cm and filling at the right side of the top plane: (a) $v=0.1$ m/s and (b) $v=0.2$ m/s

VI. RESULT AND DISCUSSION

A. The Effect of Inlet Velocity on Solidification

The effect of inlet velocity on the solidification in casting process is discussed in this section. The temperature contour for whole cavity (size of cavity: $5 \times 5 \times 5$ mm³) at different inlet velocity (v_i), for the constant time and constant pouring or inlet temperature ($T_i = 973$ K) when all walls are insulated except the left wall, is given in Fig. 5.

Fig. 5 shows the temperature contour at different velocity for the time (t) of 10 second. As increased the velocity from 0.05 m/s to 0.1 m/s, the temperature contour get more uniform as given in Figs. 5 (a) and (b). On further increased in velocity, the filling process occur faster but solidification occur later which increase the thermal arrest time. The time of thermal arrest is short when inlet velocity is low. Higher growth rate is observed for low inlet velocity as the strength of residual flow get reduces. This also results in less fluctuation in the temperature gradient at the solidifying interface

[5]. Further increase in velocity from 0.15 to 0.2 m/s, the temperature contour is not uniform as we get for the velocity 0.1 m/s given in Figs. 5 (c) and (d). At the lower part of cavity, the flow gets disturbed because of increase in turbulence. The turbulence is increased as the increase in velocity and stop after the complete filling process. This causes the porosity defect in the casting as discussed in [14]. The liquid metal in the upper part solidifies faster than in the lower part due to the cold upstream flow near the left mold wall. In the upper part, the progress of solidus line is retarded due to the secondary flow shown in Fig. 5. Secondary flow develops because of filling and buoyancy driven flow [1].

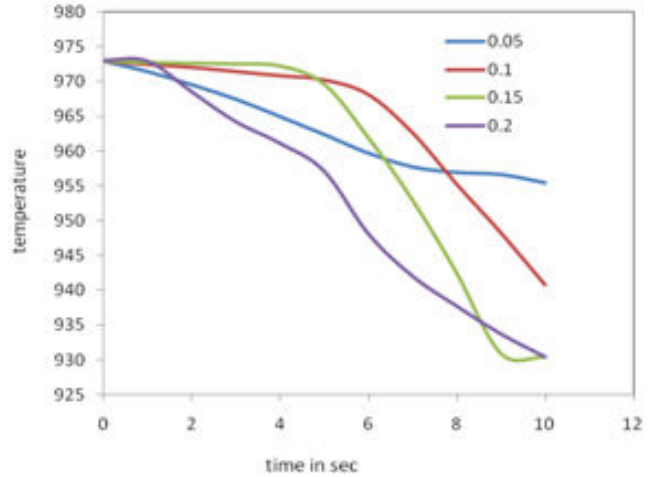


Fig. 7 Variation of temperature with time at different inlet velocity for $t = 10$ sec, $T_i = 973$ K, $T_{wl} = 773$ K, $h_g = 5$ cm and filling at the right side of the top plane

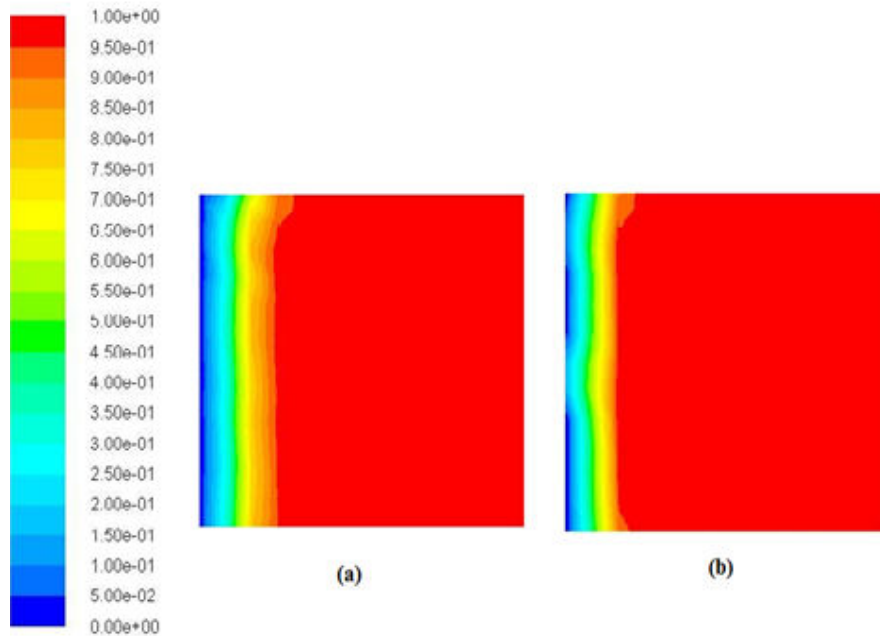


Fig. 8 Liquid fraction contour at different inlet velocity for $t = 10$ sec, $T_i = 973$ K, $T_{wl} = 773$ K, $h_g = 5$ cm and filling at the right side of the top plane (a) $v = 0.1$ m/s and (b) $v = 0.2$ m/s

The velocity contour for inlet velocity at 0.1 and 0.2 m/s for 10 sec and for constant pouring temperature (973K) is given in Fig. 6. The uniform velocity profile is found at low velocity as in Fig. 6 (a) while compare to 0.1 m/s inlet velocity, non-uniform contour is shown in Fig. 6 (b) at inlet velocity = 0.2 m/s. Therefore, velocity behavior shows the similar nature as discussed in temperature contour in Fig. 5. The non-uniform behavior is caused the cavities in casting. These cavities produce the porosity defect in casting. The variation of temperature with time at different inlet velocity of molten metal is given in Fig. 7. The increase in velocity from 0.05 to 0.2 m/s the slope of temperature with time is changed as in Fig. 7. The increased in velocity from 0.05 to 0.15 slope of the temperature decreases with increase in velocity. It suggested

that the time required for the solidification process increases. Therefore, the behavior of casting changed due to change in material properties. Further, at highest velocity (0.2 m/s), suddenly drop in temperature suggested the time required for solidification is low compare to other velocity. This is due to high turbulence behavior as discussed in Fig. 6. Therefore, high velocity entrapped more gases and inclusion melted in the molten material. Those inclusion and gases appears on the sample surface at high pouring rate pressurizes them outside the material body, so they appear on surface. Moreover, high pouring rate may mean turbulent flow which hits the mold cavity harder and result in rough surfaces as discussed by [6]. Because the velocity has an opposite effect on surface and sub-surface defects, a compromise must be made to attain the

optimum pouring rate and depending on application. If the inlet velocity is too high then it can result turbulence and if it is too low then metal solidify even before the filling completed. The liquid fraction of the both configuration are shown in Fig. 8 for the same time duration (10 sec). The solidification in first configuration (as in Fig. 8 (a)) is uniformly proceeding from layer to layer than the second

configuration as in Fig. 8 (b). It is also supporting the same behavior as discussed in Figs. 5 (b), (d) and 6. Therefore, first configuration is more appropriate for mold cavity.

B. Effect of Heat Transfer Coefficient on Solidification

The effect of heat transfer coefficient on the solidification in casting process is discussed in this section.

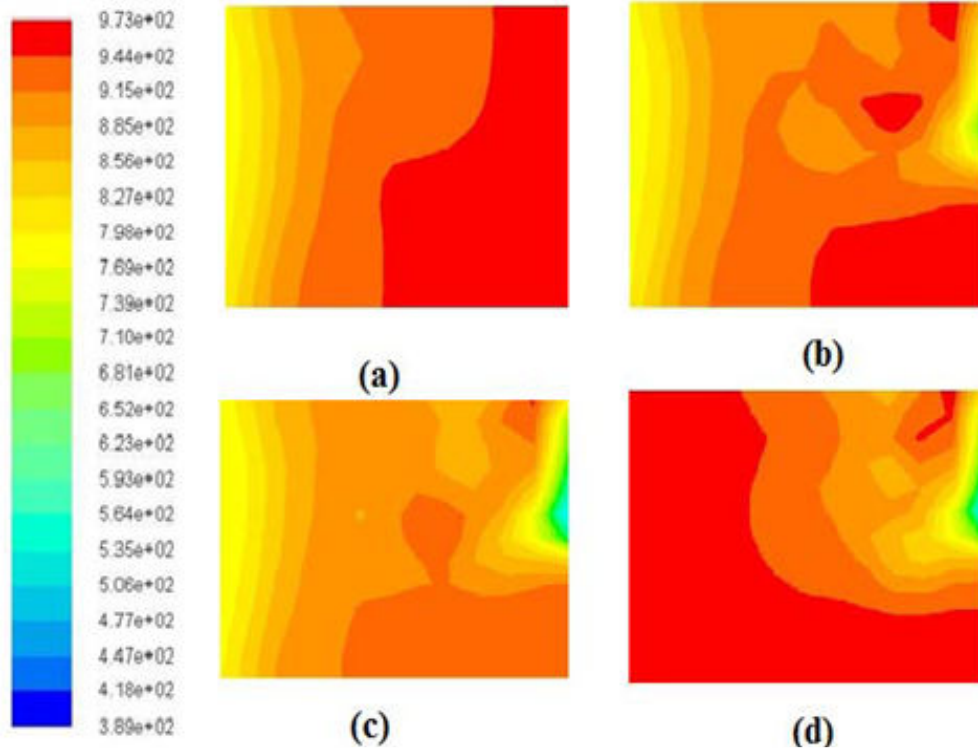


Fig. 9 Temperature contour at different heat transfer coefficient for $t = 10$ sec, $v_i = 0.1$ m/s, $T_i = 973$ K, $T_{wl} = 773$ K, $h_g = 5$ cm and filling at the right side of the top plane: (a) insulated wall, (b) 10 W/m²K, (c) 20 W/m²K and (d) 30 W/m²K

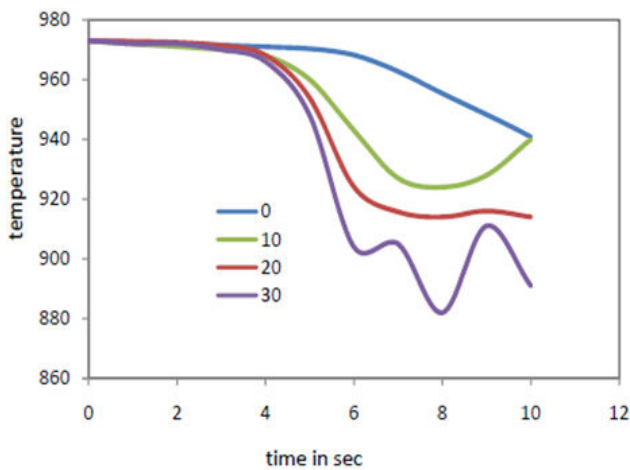


Fig. 10 Temperature variation with time at different heat transfer coefficient at the centre of mold cavity for $t = 10$ sec, $v_i = 0.1$ m/s, $T_i = 973$ K, $T_{wl} = 773$ K, $h_g = 5$ cm and filling at the right side of the top plane

Fig. 10 shows the temperature drop with time at different heat transfer coefficient. At insulated wall ($h=0$), the

temperature drop at slow rate, while in non-insulated wall, the temperature drops more quickly. The velocity contour for the insulated and high heat transfer coefficient ($h=20$ w/m²K) is shown in Fig. 11. It is also supporting the effect of cooling rate on the velocity profile. In insulated case, velocity profile is more uniform than the non-insulated case ($h=20$ w/m²K). Therefore, the possibility of defect in non-insulated case is more. The slow rate of cooling promotes crystallization whereas a faster cooling rate may prevent crystallization. Hence, the faster rate of cooling promotes the defects in casting as discussed in Fig. 7. The liquid fraction of the both configuration are shown in Fig. 12 for the same time duration (10 sec). The solidification in first configuration as in Fig. 12 (a) is uniformly proceeding from layer to layer as in second configuration in Fig. 12 (b). It is also supporting the same behavior but the temperature and velocity contours in Figs. 9 and 11 respectively suggested the possibility of defect due to non-uniform profile because of loss of heat from the other side of wall.

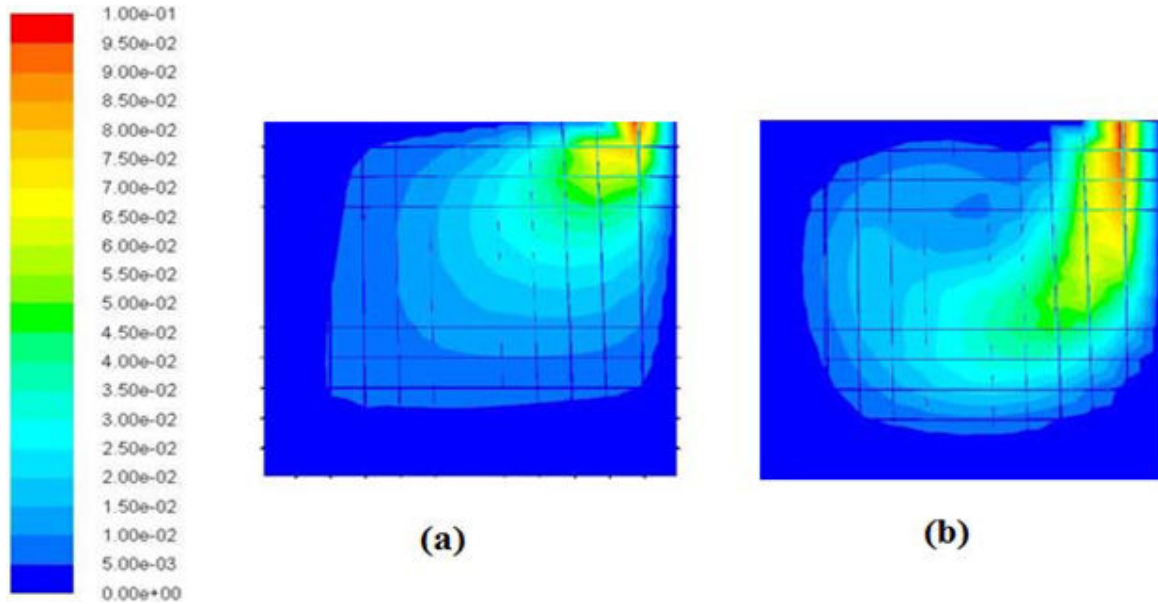


Fig. 11 Velocity contour at different heat transfer coefficient for $t = 10$ sec, $v_i = 0.1$ m/s, $T_i = 973$ K, $T_{wl} = 773$ K, $h_g = 5$ cm and filling at the right side of the top plane: (a) insulated wall and (b) $h=20$ w/m²K

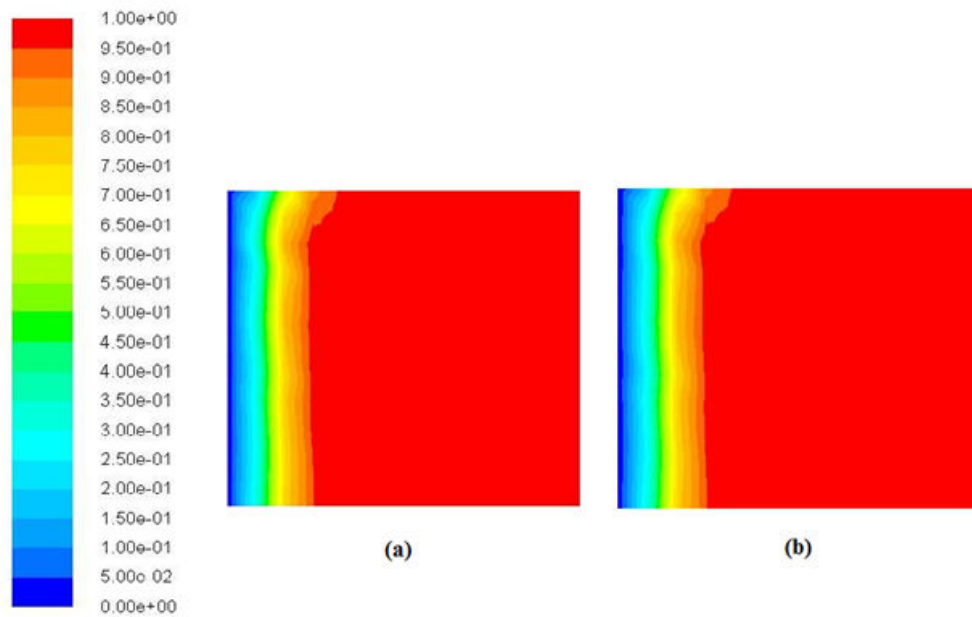


Fig. 12 Liquid fraction contour at different heat transfer coefficient for $t = 10$ sec, $v_i = 0.1$ m/s, $T_i = 973$ K, $T_{wl} = 773$ K, $h_g = 5$ cm and filling at the right side of the top plane (a) insulated wall and (b) $h=20$ w/m²K

The temperature contour at different heat transfer coefficient is given in Fig. 9. The all wall of the geometry are insulated (no transfer of heat from mould cavity to the surrounding) except left wall (to initiates the solidification). The temperature contour shown in Fig. 9 is obtained with uniform temperature distribution. While in Figs 9 (b)-(d), allowed the heat from mold cavity to the surrounding at different heat transfer coefficient ($h=10, 20, 30$ w/m²K) for the same condition. The temperature profiles are changed with heat transfer coefficient. The temperature profile of insulated case is more uniform compare to non-insulated while other

conditions remain same as shown in Fig. 9. Therefore, it is necessary to have uniform temperature profile for better solidification in layer, because it prevents the formation of defects. As the filling progresses to fill the entire mold cavity, the mold starts to become heated as well as the central casting remains much hotter than the outer casting region due to heat transfer from cavity to the surrounding (outside). The outside castings solidify quicker than the inside ones. Therefore, possibility of defects and non-uniform material properties in casting material is formed.

VII.CONCLUSION

The conclusions from the present study can be summarized as follows:

- The inlet velocity has an important effect on solidification process. On increasing the velocity, velocity distribution inside the cavity changed from uniform to non-uniform profile. Suggested the turbulence behavior inside the casting. Therefore, entrapped more gases and inclusion melted in the molten material and leads the formation of defects.
- Temperature as well as velocity profile inside the cavity shows the similar behavior. Therefore, the uniform distributions of both parameters are helpful to suggest the proper solidification process in the casting.
- The uniform temperature as well as velocity profile advice for formation of uniform liquid fraction during solidification process.

All parameters have different effect on the solidification. Therefore, it needed to make a compromise to get the optimum condition.

REFERENCES

- [1] I. T. Im, W. S. Kim and K. S. Lee, "A unified analysis of filling and solidification in casting with natural convection," International Journal of Heat and Mass Transfer, Vol. 44, pp. 1507-1515, 2001.
- [2] C. R. Swaminathan and V. R. Voller, "A General Enthalpy Method for Modeling Solidification Process," Metall Trans, Vol. 23B, pp. 651-664, 1992.
- [3] Y. Chen, Y. T. Im and J. Yoo, "Finite element analysis of solidification of aluminum with natural convection," Journal of Materials Processing Technology, Vol. 52, pp. 592- 609, 1995.
- [4] C. R. Swaminathan and V. R. Voller, "A time-implicit filling algorithm," Appl. Appl. Math. Modelling, Vol. 18, pp. 101-108, 1994.
- [5] N. Pathak, A. Kumar, A. Yadav and P. Dutta, " Effects of mould filling on evolution of the solid-liquid interface during solidification," Applied Thermal Engineering, Vol.29, pp. 3669-3678, 2009.
- [6] W. M. A. Jadayil, "Studying the Effects of Varying the Pouring Rate on the Casting Defects Using Nondestructive Testing Techniques," Jordan Journal of Mechanical and Industrial Engineering, Vol.5 pp. 521-526, 2011.
- [7] D. Vander Boon, "Effects of Solidification Rate on Porosity Formation and Cast Microstructure in Aluminum Alloy A356," Laboratory Module 3 EGR 250 – Materials Science & Engineering, February 2005.
- [8] D. Kakas, L. Kovacevic and T. Pal, "Improvement of casting process control by computer simulation and experimental observation," Proceedings of the 3rd International Conference on Manufacturing Engineering, Greece, October 1-3, 2008.
- [9] V. Gopinath and N. Balanarasimman, "Effect of Solidification Parameters on the Feeding Efficiency of Lm6 Aluminium Alloy Casting," IOSR Journal of Mechanical and Civil Engineering, Vol. 4, Issue 2, PP. 32-38, 2012.
- [10] C. J. Kim and M. Kaviany, "A fully implicit method for diffusion-controlled solidification of binary alloys," Inr. J. Heat Mass Transfer, Vol. 35, PP. 1143-1154, 1992.
- [11] M. A. Radyand A. K. Mohanty, "Natural convection during melting and solidification of pure metal in a cavity," Numerical heat transfer, Vol. 29, pp. 49-63, 1996.
- [12] J. H. Kuo, R. J. Weng and W. S. Hwang, "Effects of Solid Fraction on the Heat Transfer Coefficient at the Casting/Mold Interface for Permanent Mold Casting of AZ91D Magnesium Alloy," Materials Transactions, Vol. 47, pp. 2547- 2554, 2006.
- [13] K. Akihiko and K. Yasunori, "Mold Filling Simulation for Predicting Gas Porosity," H Engineering Review. Vol. 40, pp. 83-88, 2007.
- [14] D. K. Nguyen and S. C. Huang, "Analysis the Effects of Turbulence Flow, the Heat, and Phases Transfer on Thermal Arrest Time in Casting Process by Computational Fluid Dynamic Method," Journal of Engineering Technology and Education, Vol. 9, pp. 436-450, 2012.
- [15] A. B. Crowley and J. R. Ockedon, "On the Numerical Solution of an Alloy Solidification Problem," Int. J. heat Mass Transfer. Vol. 22, pp. 941-946, 1979.
- [16] M. Mbaye and E. Bilgen, "phase change process by natural convection-Diffusion in rectangular enclosure," Heat and Mass Transfer Vol. 37, pp. 35-42, 2001.
- [17] ANSYS, Release 14.0 UP20111024, Copyright 2011 SAS IP, Inc.